



HAL
open science

Multi-cation exchanges involved in cesium and potassium sorption mechanisms on vermiculite and micaceous structures

Julien Dubus, Nathalie Prat-Leonhardt, Christelle Latrille

► **To cite this version:**

Julien Dubus, Nathalie Prat-Leonhardt, Christelle Latrille. Multi-cation exchanges involved in cesium and potassium sorption mechanisms on vermiculite and micaceous structures. *Environmental Science and Pollution Research*, 2022, <https://doi.org/10.1007/s11356-022-22321-4>. 10.1007/s11356-022-22321-4 . cea-03770057

HAL Id: cea-03770057

<https://cea.hal.science/cea-03770057>

Submitted on 22 Jan 2024

HAL is a multi-disciplinary open access archive for the deposit and dissemination of scientific research documents, whether they are published or not. The documents may come from teaching and research institutions in France or abroad, or from public or private research centers.

L'archive ouverte pluridisciplinaire **HAL**, est destinée au dépôt et à la diffusion de documents scientifiques de niveau recherche, publiés ou non, émanant des établissements d'enseignement et de recherche français ou étrangers, des laboratoires publics ou privés.

Multi-cation exchanges involved in cesium and potassium sorption mechanisms on vermiculite and micaceous structures

Julien Dubus

French Alternative Energies and Atomic Energy Commission Saclay: Commissariat a l'Energie Atomique et aux Energies Alternatives Centre de Saclay

Nathalie Leonhardt

French Alternative Energies and Atomic Energy Commission: Commissariat a l'Energie Atomique et aux Energies Alternatives

Christelle Latrille (✉ christelle.latrille@cea.fr)

French Alternative Energies and Atomic Energy Commission Saclay: Commissariat a l'Energie Atomique et aux Energies Alternatives Centre de Saclay

Research Article

Keywords: Cesium, cation exchange, interlayer collapse, vermiculite, potassium

Posted Date: April 20th, 2022

DOI: <https://doi.org/10.21203/rs.3.rs-1484971/v1>

License:   This work is licensed under a Creative Commons Attribution 4.0 International License.

[Read Full License](#)

Abstract

Vermiculite and micaceous minerals are relevant Cs sorbent in soils and sediments. To understand Cs bioavailability in soils resulting from multi-cation exchanges, Cs sorption onto clay minerals have been carried out in batch experiments with solutions containing Ca^{2+} , Mg^{2+} and K^+ . A sequence between a vermiculite and various micaceous structures were achieved by conditioning a vermiculite at various amounts of K. Competing cation exchanges were investigated according to the concentration of Cs. The contribution of K on trace Cs desorption is probed by applying different concentrations of K on Cs-doped vermiculite and micaceous structures. Cs sorption isotherms at chemical equilibrium were combined with elemental mass balances in solution and structural analyses. Cs replace easily $\text{Mg}^{2+} > \text{Ca}^{2+}$ and competes scarcely with K. Cs is strongly adsorbed on the various matrix and a K/Cs ratio about a thousand is required to remobilize Cs. Cs is exchangeable as long as the clay interlayer space remains open to Ca^{2+} . However, excess of K, as well as Cs, in solution leads to the collapse of the interlayer spaces that locks the Cs into the structure. Once K and/or Cs collapse the interlayer space, the external sorption sites are then particularly involved in Cs sorption. Subsequently, Cs^+ exchanges preferentially with Ca^{2+} rather than Mg^{2+} . Mg^{2+} is extruded from the interlayer space by Cs^+ and K^+ adsorption, excluded from short interlayer space and replaced by Ca^{2+} as Cs^+ desorbs.

1. Introduction

Subsequently to the nuclear contamination in the Fukushima prefecture, numerous studies have been dedicated to the understanding of radiocesium mobility to predict their impact in the environment and so to anticipate potential risks on health (Klika et al. 2007; Nakao et al. 2014; Liu et al. 2004; Kasar et al. 2020; Siroux et al. 2021). To counteract the bioavailability of cesium in soils, K fertilization was recommended in Japan (Kato et al. 2015) to deplete Cs incorporation by plants by acting on competing rule between Cs and K in plants as well as in soils (Kato et al. 2015; Kubo et al. 2015, 2017). Nevertheless, Cs transfer to plant is highly dependent on the clay mineralogy, especially as soils are enriched in micaceous minerals and vermiculite (Kubo et al. 2018). Weathering micaceous minerals are able to release K^+ to reduce Cs^+ uptake by plants. On the other hand, biotite, vermiculite, and aluminous smectite are known to adsorb strongly Cs^+ compared to other cations (Sakalidis 1988; Cornell 1993; Maes et al. 1999; Mukai et al. 2016; Durrant et al. 2018; Wissocq et al. 2018; Ogasawara et al. 2019; Kitayama et al. 2020). Moreover, illite and partially-vermiculitized biotite sorb Cs^+ more strongly than vermiculite (Sawhney 1972; Brouwer et al. 1983; Maes et al. 1999; Kitayama et al. 2020; Latrille and Bildstein 2022). Indeed, these clay minerals provide selective sorption sites that enhanced Cs sorption (Brouwer et al. 1983; Park et al. 2019), which appear in some instances as Cs fixation sites (Kikushi et al. 2015). Cs^+ sorption is mainly controlled by an ion exchange process on clay mineral surfaces (Mishra et al. 2015).

Due to isomorphic substitutions in tetrahedral and octahedral layers and hydroxyl groups with amphoteric character at the particle edges, these minerals hold different types of sorption sites. Generally, sorption sites are structurally located on the basal planes of the phyllosilicate layer, on the crystal border

and in the interlayer space. Weathered micaceous minerals and especially illite exhibit frayed edges which refer to the transition zones between collapsed and open interlayer space. Since Sawhney (1972), particular reactive properties have generally been attributed to this specific space. Due to its configuration, it can accept only low hydration energy cations or small size cations including K^+ and Cs^+ compared to Ca^{2+} and Mg^{2+} . Moreover, Cs^+ can deeply penetrate inside the closed interlayer space by ion-exchange (Kogure et al. 2012; Okumura et al. 2018).

The adsorption process depends on Cs concentration, solution ionic-strength, competing cation and pH (Fuller et al. 2014; Missana et al. 2014). This involves the compensating cation placed on the negative surface charges of phyllosilicates and cations in solution. At trace concentration, Cs^+ is easily replaced by Mg^{2+} (Morimoto et al. 2012; Tamura et al. 2015) on vermiculite, whereas Cs is stronger adsorbed on illite (Wissocq et al. 2018) but remains exchangeable (Latrille and Bildstein 2022). At high Cs concentration, it has been assumed that weakly hydrated Cs^+ sorbed to the frayed-edges of micaceous minerals is dehydrated which results in a partial collapse of the interlayer (Mukai et al. 2016; Sawhney 1972; Kikuchi et al. 2015; Park et al. 2019). Likewise, Cs incorporated in the vermiculite interlayer by ion exchange with Mg^{2+} , Ca^{2+} and Na^+ , induces subsequent interlayer collapse in vermiculite (Sawhney 1972; Lee 1973, 1974; Kogure et al. 2012; Dzene et al. 2015; Yin et al. 2017; Kitayama et al. 2020). Cesium trapped in the interlayer space is consequently excluded from desorption (Kogure et al. 2012; Motokawa et al. 2014a, b; Yamamoto et al. 2019) or is poorly displaced by hydrated divalent cations (Sawhney 1964; Yin et al. 2017). Only adsorbed Cs on planar and edge sites remain exchangeable (Dzene et al. 2015; Yin et al. 2017).

The Cs^+ sorbed to micaceous minerals are generally weakly exchanged by competitive cations such as K^+ and NH_4^+ (Liu et al., 2004; Ohnuki and Kozai, 2013) despite their similar chemical properties. This indicates that the minerals are more selective for Cs^+ than K^+ and NH_4^+ . NH_4^+ extracts smaller amounts of Cs than hydrated Mg^{2+} and Ca^{2+} ; K^+ is the most efficient compared to the other cations (Yin et al. 2017). Furthermore, dehydrated K^+ originally in the interlayer space of micaceous minerals remains non exchangeable in contrast to those of expanding phyllosilicate. Only the weathering process partially releases interlayer cations from micas (Benedicto et al., 2014; Sawhney, 1972). Then, superimposed to chemical ion-exchange, a physical mechanism leads to the capture of cations at low hydration potential into the mineral. Competition between K^+ and Cs^+ is associated with their location in the mineral structure and Cs sorption properties of micaceous minerals differ according to their degree of weathering (Kitayama et al. 2020; Murota et al. 2020). Consequently, sorption properties of pristine minerals deviate from those which are weathered in soils.

To understand bioavailability of radionuclides in soils, knowledge of sorption-desorption behavior in soil-water systems remains crucial (Kasar et al. 2020). At chemical equilibrium, the reversibility of the adsorption process can be validated by desorption respecting the same physico-chemical condition. However, Cs desorption properties of clay minerals are frequently deduced from forced ion-exchange accounting chemical extractants (Brouwer et al. 1983; Dzene et al. 2015; Yin et al. 2017; Mukai et al.

2018; Kitayama et al. 2020; Murota et al. 2020), which qualifies a different reactional pathway than the adsorption process. The partitioning between solid and solution, usually named K_d , is finally recommended to verify the adsorption reversibility (Wissocq et al. 2018; Kasar et al. 2020). The K_d value of adsorption and desorption have to be aligned on the concentration isotherm. This implies control of the chemical exchange at equilibrium by respecting the mass action law and thus the cation mass balance in the system. Cs sorption on clay mineral is often studied in single cation pair exchange or far from a natural context. Although cation adsorption/desorption depends on competitions with surrounding cations in solution, especially major cations, few studies have been focused on Cs sorption competing simultaneously with several cations in soil solution (Kasar et al. 2020).

The aim of this study is to further understand the Cs adsorption and desorption behavior on micaceous minerals and vermiculite in chemical environment close to a natural soil. In order to mimic the transition between weathered mica and vermiculite, a vermiculite was K saturated at various degree of interlayer closing. Their exchange properties were then controlled. Finally, Cs adsorption/desorption behavior is investigated in multi-cation solutions. This involves simultaneous Cs^+ competition with Ca^{2+} , Mg^{2+} and K^+ . Cesium concentration isotherms are acquired in batch experiments performed in controlled physico-chemical conditions at thermodynamic equilibrium. Desorption experiments performed with the same cation species allow to test the Cs adsorption reversibility. Cation mass balances are checked for each chemical condition to highlight cation competitions and selectivities occurring during Cs sorption. Then K^+ competition on Cs^+ desorption is studied by imposing various amounts of K on trace Cs doped vermiculite and K intercalated vermiculite. K^+ concentrations were selected to mimic a K amendment in the fields, a K depletion in the solution due to plant uptake or weathering event, and to provide insight into the Cs location in the mineral structure. Subsequent chemical disturbance in solution were recorded through cation mass balances. Finally, chemical results coupled with structural analyses by XRD lead to propose a reactional scheme for Cs adsorption and desorption in multi-cations solutions. Structural localization of sorption sites is addressed and discussed.

2. Materials And Methods

2.1. Materials and conditioning process

A commercial vermiculite (Sigma Aldrich) was selected for this study. The chemical analysis of the raw vermiculite gives the following structural formula

$(Si_{2.905}Al_{1.021}Fe_{0.075})(Fe_{0.311}Mg_{2.624}Ti_{0.06})O_{10}(OH)_2K_{0.204}Ca_{0.034}Mg_{0.201}$. XRD analysis revealed a pristine vermiculite associated with a vermiculite/mica mixed layer. CEC determined by NH_4 exchange at pH 7 is 109.6 ± 1.2 meq/100g compared to the theoretical CEC estimated to 166 meq/100g. The non-exchangeable K by NH_4 is consistent with a mixed layer vermiculite/mica. Raw vermiculite was initially finely crushed and suspended in ultrapure water for one night, sonicated in a tank and sieved to isolate the 25 – 20 μm particles. Conditioning and experiment solutions were prepared by dissolving salt

and their dilution with ultrapure water (milli-Q, 18.2 MΩ.cm⁻², Millipore®). Salts of KCl (VWR Chemical), Ca(NO₃)₂ 4H₂O (VWR Chemical), Mg(SO₄) 7H₂O (VWR Chemical), Mg(NO₃)₂ 6H₂O (VWR Chemical) were used. Acidification was done with ultrapure nitric acid (Chem-Lab) and phosphoric acid (Sigma Aldrich) diluted at appropriate concentrations when needed. The 20–25 μm vermiculite fraction was partitioned in five batches, each conditioned with five solutions remaining to 2.5 10⁻² mol/L Ca and 3.75 10⁻² mol/L Mg and varying by their K concentrations at 0, 0.125, 1.25, 6.25 and 12.5 10⁻² mol/L K. Batches of 1.5 g of vermiculite were dispersed in 120 mL of solutions with a 12.5 g/L solid/solution ratio, end to end shaken for three days and centrifuged at 10596 *g* during 40 min to replace the supernatant by the same conditioning solution. These operations were repeated three times. Three similar operations were successively realized with the same solution composition diluted 12.5 times, named K(x) solution (x = 0, 0.1, 1, 5 or 10) with cation composition detailed in Table 1, in order to equilibrate the solids with operating solutions. The solids were finally rinsed with ethanol to eliminate residual salt. After centrifugation, the five conditioned materials were left to air-dry for two days.

Table 1
Cation composition of K(x) solutions

solution	Ca²⁺ (10⁻³ mol/L)	Mg²⁺ (10⁻³ mol/L)	K⁺ (10⁻³ mol/L)
K(0)	2	3	0
K(0.1)	2	3	0.1
K(1)	2	3	1
K(5)	2	3	5
K(10)	2	3	10

Cation exchange capacities (CEC) of conditioned vermiculites are deduced from compensating cations exchanged by NH₄ at pH 7. Firstly, 50 mg of dried conditioned vermiculite was dispersed in 4 mL of 0.1 mol/L NH₄Cl, end to end shaken for one week and centrifuged at 33000 *g* during 40 min. Cation concentrations of supernatants were analyzed by ionic chromatography and low K concentrations were refined by ICP-AES (Activa, Horiba Jobin Yvon) measurements.

2.2. Cs adsorption/desorption at equilibrium

The effects of Cs concentration were investigated by sorption isotherms for each conditioned vermiculite following the approach described in Wissocq et al. (2017) and Siroux et al. (2021). For all these batch experiments, 70 mg of dried conditioned vermiculite was dispersed in 6.1 mL of K(x) solution, leading to a solid/solution of 11.4 g/L. Each batch suspension was spiked with ¹³⁷Cs by adding 30 μL of a source (¹³⁷CsCl in HCl 0.1 mol/L) containing an activity of 7000 Bq, corresponding to 4.6 10⁻⁸ mol/L of Cs introduced. For higher concentrations required, stable isotope (CsCl solution, Fluka Ultra) were added to

achieve a solute concentration ranged between 10^{-7} and 10^{-2} mol/L. Protons introduced by radiotracer were compensated by the addition of deaerated 0.02 mol/L $\text{Ca}(\text{OH})_2$ solution freshly prepared. The pH was naturally buffered by conditioned vermiculites and checked. Suspensions were orbital shaken during 14 days, sufficient contact time to reach chemical equilibrium (based on Dzene et al. (2015) study and checked by kinetics measurement in SI1), and centrifuged at 33000 *g* (Beckman Optima LE-80K Ultracentrifuge) for 45 min. The supernatants were collected for electrolyte concentration analysis, ^{137}Cs counting and to check the pH at equilibrium.

Desorption experiments were carried out on the slurry resulting from the adsorption step. $\text{K}(\text{x})$ solutions were used to exchange Cs^+ with cations in solutions respecting pH, solid/solution ratio and contact time used in the adsorption step. Activity from the residual adsorption solution not recoverable from the slurry, was taken into account to define the initial adsorbed ^{137}Cs activity of the vermiculites for desorption step. ^{137}Cs and cations (Ca^{2+} , Mg^{2+} , K^+) in solution were analyzed by gamma counting and ion chromatography respectively, on supernatants collected after a new centrifugation cycle. Total Cs concentration is deduced from ^{137}Cs activity by assuming no isotopic fractionation between ^{137}Cs and ^{133}Cs , as previously verified by Wissocq et al. (2018). Moreover, no natural Cs amount was measured on raw vermiculite. pH was also checked at equilibrium.

The effects of K^+ concentrations on Cs^+ desorption were investigated by batch experiments on conditioned vermiculites with $\text{K}(0)$ and $\text{K}(5)$ solutions doped in ^{137}Cs at $7.6 \cdot 10^8$ mol/L ($6.62 \cdot 10^{-6}$ mol/kg of adsorbed Cs). For that, 70 mg of dried conditioned and doped vermiculite was dispersed in 6 mL of $\text{K}(0)$ solution added of KCl solutions. For vermiculite exempt of K (in $\text{K}(0)$), the introduced KCl concentrations were ranged between $3 \cdot 10^{-6}$ mol/L and $5.9 \cdot 10^{-2}$ mol/L whereas KCl concentrations were ranged between $1.5 \cdot 10^{-4}$ and $4.9 \cdot 10^{-2}$ mol/L for conditioned vermiculite with $\text{K}(5)$. The suspensions were orbital shaken during 14 days and centrifuged as above described. The supernatants were collected for electrolyte concentration analysis, ^{137}Cs counting and to check the pH at equilibrium.

Aqueous cation concentrations were measured by ion chromatography (standards Chem-Lab). The measurement uncertainties were $5 \cdot 10^{-6}$ mol/L 2σ (i.e 10^{-6} eq). The radioactivity of 1 ml supernatant was measured by gamma counting (Perkin Elmer Wizard 3). pH values were determined using a combined glass pH electrode (Mettler Toledo) equipped with an Ag/AgCl reference electrode. The electrode was calibrated with buffer solutions at pH 4.0, 7.0 and 12.0. Uncertainties were calculated by error propagation and established at ± 0.2 pH unit.

Cations adsorption and desorption by exchange with cations in solution at chemical equilibrium are expressed by:

$$m\left\{\left(\text{X}_i^-\right) - \text{N}^{n+}\right\} + n\text{M}^{m+} = n\left\{\left(\text{X}_i^-\right)_m - \text{M}^{m+}\right\} + m\text{N}^{n+}$$

with $(X_i^-) - N^{n+}$ and $(X_i^-) - M^{m+}$ the adsorbed cations on the X_i^- sorption sites, and M^{m+} and N^{n+} , the cations in solution. These reactions are described by the apparent exchange constants according to the mass action law, such as:

$$K_{N^{n+} / M^{m+}}^* = \frac{[(X_i^-)_m - M^{m+}]^n [N^{n+}]^m \gamma_{N^{n+}}^m}{[(X_i^-)_n - N^{n+}]^m [M^{m+}]^n \gamma_{M^{m+}}^n} = 1 / K_{M^{m+} / N^{n+}}^*$$

where K^* is the apparent exchange constants, i is the type of sorption site, $[\]$ is the concentration of species in solution (mol/L) or sorbed species (mol/kg of dry solid) and γ is the activity coefficient of species in solution.

Both Cs adsorption and desorption isotherm results were expressed in terms of distribution coefficient K_d , which is defined by the ratio of the adsorbed Cs concentration ($[Cs]_{ads,eq}$ in mol.kg⁻¹) over the Cs concentration in solution ($[Cs^+]_{sol,eq}$ in mol.L⁻¹). Thanks to ¹³⁷Cs radioisotope, K_d can be also estimated by the Cs activity initially introduced (A_{ini} in Bq) and measured in solution at equilibrium ($A_{sol,eq}$ in Bq).

$$K_d = \frac{[Cs]_{ads,eq}}{[Cs^+]_{sol,eq}} = \left(\frac{[Cs]_{ini}}{[Cs^+]_{sol,eq}} - 1 \right) = \left(\frac{A_{ini}}{A_{sol,eq}} - 1 \right) \frac{V}{m}$$

Mass balance expressed the variation of the chemical composition that occurred in solution during the cation exchange process. Each cation concentration in solution was converted to equivalent of cation (mole of positive charge) in the system. Mass balance in each batch (Δeq) was therefore calculated by the equivalent of cation at equilibrium in solution subtracted from the equivalent of cation initially introduced by the K(x) solutions. For adsorption experiments, the introduced solutions K(x) were added with Cs whereas for desorption experiments, the K(x) solutions are free of Cs. Negative values express an uptake onto the solid. Conversely, positive values represent a release into the solution.

Experimental errors were hence calculated for each batch following the propagation errors theory. The variance of a G function of different x_j variable can be calculated from the variances of the variables x_j using this expression:

$$\sigma_G^2 = \sum_{i=1}^n \left(\frac{\partial G}{\partial x_i} \right)^2 \sigma_i^2 + 2 \sum_i \sum_j \frac{\partial G}{\partial x_i} \frac{\partial G}{\partial x_j} \sigma_{ij}$$

where $(\partial G / \partial x_j)$ is the partial derivative of G with respect to x_j , σ^2 is the variance of x_j and σ_{ij} the covariance of the x_j and x_j variables. If these variables are independent, the covariance term is then equal to zero.

2.3. Crystal-structure analysis

X-ray diffraction (XRD) analyses were performed using a XRD 5000 INEL powder X-ray diffractometer using Cu K α radiation, equipped with a CPS120 curve detector Si/Li. The XRD patterns were scanned between 3° and 110° 2 θ angle at 30 kV and 30 mA with a Cu-target tube at room temperature of 22°C. Patterns were cumulated every few seconds during 10 minutes. Analyses were performed on oriented clay deposits to characterize the cation exchanges that occur in the interlayer space. The peak for (001) reflection was scanned to detect shifts due to occupancy change (Yin et al. 2017). This reflection gives the interlayer distance of vermiculite structures. Basal spacings ($d_{(001)}$) are ranged between 14.3 Å to 14.9 Å for mixed interlayer occupancy by Ca and Mg, whereas $d_{(001)}$ spacing is reduced to 10.4 Å for K occupancy or 10.8 Å to 11.4 Å for Cs occupancy in vermiculite (Brindley and Brown 1980; Dzene et al. 2015; Kogure et al. 2012). For this purpose, the XRD patterns were recorded on samples resulting from Cs desorption experiments. Vermiculite slurries were dispersed in pure water, dropped on glass slides and air dried to obtain oriented preparations.

3. Results And Discussion

3.1. Exchange capacity of conditioned vermiculites

The conditioning of vermiculites with various K(x) solutions leads to impose the composition of compensating cations on vermiculite negative charges. Moreover, it permits to select various intercalated K structures in a sequence between vermiculite and depleted K micaceous structures. The analyses of the cations extracted with NH₄Cl at pH 7 were performed on each conditioned vermiculite. The sum of these exchangeable cations leads to the CEC (Table 2). The vermiculite conditioned with the K-free solution (K(0)V) indicates the highest CEC at 127 cmol(+)/kg. The K is largely extracted from the original vermiculite by the conditioning process. This is controlled by XRD analysis that shows a (001) reflection with a d -value at 14.6 Å indicating a major di-hydrated Ca, Mg occupancy in the interlayer space (Fig. 1). As K⁺ increases in the conditioning solutions, decreases of the CEC of the conditioned vermiculites is observed. Indeed, K⁺ appears very difficult to extract with NH₄⁺: the exchangeable K⁺ represents less than 1% of extractable cations for K(0)V to K(5)V with a maxima at 1.4% for K(10)V. Moreover, with the increasing of the amount of K⁺ in the conditioning media, the intensity of the (001) reflection at 14.6 Å decreases and peaks open towards the large angles, while a second broad reflection appears and grows in intensity (Fig. 1). Therefore, some K⁺ are incorporated in the interlayer space of vermiculite during the conditioning process to form vermiculite/ mica mixed layers.

Based on the maximal value of CEC obtained from K(0)V (Table 2), K⁺ accounts for 11, 18, 27 and 33% of CEC for K(0.1)V to K(10)V respectively. While Mg/Ca ratios were maintained to 1.5 in each solution K(x), it decreased from 2.96 to 1.53 for the extractable cations of the structures K(0)V to K(10)V. This indicates the higher Mg²⁺ affinity of vermiculite than Ca²⁺ in the absence of K⁺. As K⁺ amount increases in the

structure, Mg^{2+} amount decreases whereas the incorporated Ca^{2+} varies slightly. Then, K^+ replaces Mg^{2+} more easily than Ca^{2+} during its incorporation into the structure (Robin et al. 2015).

Table 2
CEC and cations exchangeable compositions of vermiculites conditioned with five K(x) solutions.

Matrix	CEC	Exchangeable cations		
		Ca^{2+}	Mg^{2+}	K^+
	cmol+/kg	cmol+/kg	cmol+/kg	cmol+/kg
K(0)V	127.1	32.0	94.8	0.3
K(0.1)V	113.2	29.5	83.3	0.4
K(1)V	104.3	28.2	75.6	0.5
K(5)V	93.6	27.9	64.9	0.8
K(10)V	86.5	33.7	51.6	1.2

3.2. Cs sorption behavior on vermiculite and micaceous structure in multi-cation media

Cs adsorption and desorption isotherms (Fig. 2) were performed on the five conditioned vermiculites in function of Cs concentration in the multi-cation K(x) solutions at chemical equilibrium. Cs repartition between solid and liquid is expressed by the K_d value. Similarly, to illite and smectite, Cs adsorption on vermiculite is non-linear with the Cs concentration in solution (Durrant et al. 2018; Wissocq et al. 2018; Latrille and Bildstein 2022).

Regardless of the matrix and the solution composition, when the Cs concentration increases in solution, the Cs adsorption K_d decreases to reach a local minimum between 2 and 4 10^{-6} mol.L⁻¹, then increases to a local maximum between 0.38 and 2.4 10^{-4} mol/L Cs depending on the solution, before decreasing again at the highest Cs concentrations. The highest Cs adsorption occurs on vermiculite in K-free solution (K(0)) at Cs concentration below 2 10^{-6} and up to 10^{-5} mol/L. At Cs trace concentrations ($< 10^{-7}$ mol/L), the more the K amount in the conditioned vermiculites and their respective conditioning solution, the lower the K_d value (for K less than 1 mmol/L). Above 5 mmol/L K in the media, the K_d of Cs in trace becomes slightly larger. All matrices give a similar lowest K_d value at about 10^{-6} mol/L Cs in solution. Conversely, the highest K loaded vermiculite (K(10)V) records the lowest Cs adsorption K_d above 10^{-5} mol/L Cs.

Adsorption reversibility is verified when the apparent exchange constant for adsorption reaction is the inverse of the apparent exchange constant for desorption reaction at chemical equilibrium ($K_{ads}^* = \frac{1}{K_{des}^*}$), according to the mass action law. As major cation concentration remains constant for both reactions,

especially at low Cs concentration, Cs adsorption K_d is similar to the Cs desorption K_d (Durrant et al. 2018; Wissocq et al. 2018). This means that the desorption reaction must have released the right Cs amount in the liquid phase to reach equilibrium. This does not imply that the total amount of adsorbed Cs should be desorbed at equilibrium. At Cs concentration below 10^{-7} mol/L, Cs adsorption is reversible until 5 mmol/L of K in solution (Fig. 2). Only 4.3 to 5.6% of the adsorbed Cs is released at the desorption step. This suggests that Cs could be desorbed over an extended time period (Murota et al. 2016). For K concentration higher than 5 mmol/L, adsorption becomes partially reversible as shown by the desorption K_d slightly higher than adsorption K_d for K concentration at 10 mmol/L (K(10)). Between 10^{-7} and $5 \cdot 10^{-5}$ mol/L of Cs in solution at equilibrium, the reversible adsorption is the lowest, with very close values whatever the K concentration in the medium. At higher Cs concentration ($> 5 \cdot 10^{-5}$ mol/L), partial reversible adsorption is observed with the highest K_d of adsorption / desorption ratio for K(0)V. This ratio decreases with the K contents increase in solids and solutions. So, the Cs adsorption capacity ensured by sorption sites located in the interlayer space is reduced due to their occupancy by K, in accordance with the CEC (Table 2) and the (001) reflection distances decrease with K incorporation in the structure (Fig. 1).

These non-linear isotherms are comparable to those of illite and smectite (Wissocq et al. 2018), except the K_d increase at Cs concentration above 10^{-5} mol/L. They emphasize the involvement of several sorption sites distinguishable by their selectivity towards Cs, as seen on Ca-vermiculite (Latrille and Bildstein 2022). Referred to this latter study, at trace concentration, a low capacity and high selectivity site contributes mainly to Cs adsorption. This sorption site type records also a strong K selectivity given the decreasing K_d of Cs when K increases both in solid and solution. It is noticeable that the K concentration must be at least a thousand times higher than Cs for this competition to occur. While the capacity of this site to load Cs is saturated, the K_d of Cs decreases drastically. Thereafter, one or several low Cs affinity sites continue to take Cs up, which explains the decrease of the K_d value. At concentration above 10^{-5} mol/L, the high Cs upload may result from the presence of one or several high capacity sites. Lee (1973, 1974) and Latrille and Bildstein (2022) observed a similar trend onto Ca, Mg or Na saturated vermiculite and explained it by the penetration of Cs into the interlayer space depending on the compensating cation. In the case of several cations involved in the Cs uptake by conditioned vermiculites, the cation mass balance of the solution compositions gives the variation of element amounts in the solution compared with the initial solution K(x). As a result, this was used to evaluate the ongoing reactional processes. Focus was made on the cation mass balances obtained on adsorption and desorption solutions resulting from equilibrium between vermiculites K(0)V and K(5)V in solution K(0) and K(5) respectively (Figs. 3 and 4). Effectively, these two sorption conditions are selected to highlight two Cs adsorption behaviors depending on the rate of K intercalated in the vermiculite structure. In the initial state, compensating cations on K(0)V and K(5)V are mainly Ca^{2+} and Mg^{2+} , and K^+ appears as poorly exchangeable in both vermiculites structures (Table 2). Note that the chemical compositions of solutions K(0) and K(5) (Table 1) contain Cs at various concentrations for adsorption step whereas these solutions are initially free of Cs for desorption step. The cations mass balances evidence the Ca^{2+} , Mg^{2+} , K^+ and H^+ exchanges involved with Cs adsorption and desorption, depending on Cs concentration. They

express the Cs mobility taking into account the cations selectivity and chemical competitions. Mass balances of cations involved in cation exchanges with Cs on K(0.1)V, K(1)V and K(10)V are displayed in SI2. Significant Δ_{eq} is delimited by the quantification limit by ion chromatography and the cumulated mass balance uncertainties, fixed to 10^{-6} equivalent (+) charge for Ca, Mg and K and the experimental uncertainty to $4 \cdot 10^{-13}$ Eq. (2σ) calculated for Cs^+ .

As cation exchange with H^+ may occur for Cs sorption onto clay minerals (Wissocq et al. 2018; Durrant et al. 2018), the pH of the adsorption and desorption solutions were monitored along the isotherms at equilibrium. The pH value did not vary significantly around 5.6 (initial solutions pH) except for the adsorption experiment performed with the highest Cs concentration (SI3) in which pH falls to 5.1. However, this pH value variation, although significant, associates a negligible amount of protons that could be involved in the exchanges (i.e. $3.7 \cdot 10^{-8}$ mol of H^+) with Ca^{2+} , Mg^{2+} and K^+ . Moreover, H^+ acts slightly on Cs adsorption/desorption behavior (Latrille and Bildstein 2022) in this pH range.

At the adsorption step (Fig. 3), cations content in solution at equilibrium are compared with those of K(x) solutions doped with Cs. The Cs adsorptions on K(0)V and K(5)V at concentration below 10^{-4} mol/L Cs (Fig. 3) indicate that the solutions composition remain mainly similar to the initial solutions. The Δ_{eq} of Ca and Mg in solution are not significant (ca. $1 \cdot 10^{-6}$ eq) for K-free media whereas the significant release of Mg and Ca are of few extents (ca. $2 \cdot 10^{-6}$ eq) in media containing K. Cs adsorption in trace level does not vary significantly the cation composition of solution. Whatever the Cs amounts uptake until $2 \cdot 10^{-5}$ mol/L Cs concentration in solution, Ca and Mg tend to equally exchange with Cs. Moreover, Cs adsorbed on K(0)V is of the same amount as on K(5)V (Fig. 3). K^+ and H^+ amounts remain constant in solution whatever the Cs concentration introduced; therefore, they do not contribute in the exchange with Cs (SI2). Hence, this corroborates the fact that the K incorporated in the vermiculite structure such as K(5)V remains non exchangeable with Cs. Beyond 10^{-4} mol/L of Cs, Cs depletes largely from the solution and is compensated by $Mg^{2+} > Ca^{2+}$ desorption. Larger Cs adsorption occurs on vermiculite K-free in accordance with its larger CEC than on the K incorporated vermiculite. At the highest Cs concentration, Cs^+ compensates 74% of the K-free vermiculite CEC compared to 81% of the K incorporated vermiculite. Mass balance of cations remain equilibrated in all tested conditions. This further advocates for a cation exchange process to describe Cs adsorption. The cation exchanges observed on the intermediate K-vermiculite, K(0.1)V and K(1)V in SI2, indicate the same trends : below 10^{-4} mol/L Cs, release of Mg and Ca are of few extent and become progressively significant with increasing K in the media. This suggests easier desorption of Mg^{2+} and Ca^{2+} in presence of K^+ even though the K^+ concentration remains constant in solution. This should be related to a slight structural change which will be discussed below.

At the desorption step (Fig. 4), cation composition in solution at equilibrium is compared with those of fresh K(x) solutions. No significant adsorption of K^+ , Ca^{2+} and Mg^{2+} ($< 1 \cdot 10^{-6}$ eq) is recorded in compensation of trace Cs release. This expresses that media remains mainly at equilibrium during Cs exchange. The released Cs concentrations are too low to disturb the Ca^{2+} , Mg^{2+} and K^+ in major concentration in solution, in these experimental conditions. Moreover, trace Cs desorbed from K(0)V is of

same amount than from K(5)V. As Cs concentration becomes competitive with major cations, beyond 3×10^{-5} mol/L Cs, Cs release is accompanied by Mg^{2+} release which are compensated by Ca^{2+} adsorption for K-free vermiculite (Fig. 4a). For K intercalated structures (Fig. 4b), Cs release is mainly compensated by Ca^{2+} and to a lesser extent by K^+ ($> 1 \times 10^{-6}$ eq). This suggests a higher selectivity of site loading Cs^+ for Ca^{2+} than Mg^{2+} or a lack of site accessibility for Mg^{2+} . At high Cs concentration, the more K is initially intercalated in the structure the higher the amount of Cs desorbed. Indeed, the amount of Cs released from K(5)V (5.4% of the CEC) is greater than that from K(0)V (1.2% of the CEC) although its CEC is lower (Fig. 4 and SI2). It therefore appears that Cs desorption is easier in K intercalated than in vermiculite K-free structures. This suggests a competition between Ca and K with Cs or a structure collapse inhibiting the Cs desorption as previously observed in many studies (Kogure et al. 2012; Dzene et al. 2015; Latrille and Bildstein 2022). As intercalated K is higher in the structure, Mg^{2+} and Ca^{2+} replace Cs^+ (see K(10)V in SI2). This argues for Cs desorption from easily accessible sorption sites.

So, two Cs sorption behaviors are evidenced by chemical analyses of solutions in equilibrium with vermiculites at various K incorporation rates. As expected, K incorporated in the structure is not significantly displaced by Cs during the Cs adsorption/desorption process. Major cation composition of solutions remains stable during Cs adsorption/desorption in trace concentration due to the difference in concentration between major cations and Cs involved in the exchange. The reversible adsorption process is verified by K_d of Cs values (Fig. 2). The low ratios of Cs amounts desorbed in solution with those adsorbed reflect the high Cs selectivity towards the structures. When the Cs concentration exceeds 10^{-5} mol/L, the cation competition between Ca^{2+} , Cs^+ and Mg^{2+} takes place: Cs replaces mainly Mg^{2+} for adsorption whereas Ca^{2+} replaces mainly Cs for desorption. Cs sorption sites seem more available for cation exchange in a K incorporated structure than in a K-free structure.

3.3. K competition with Cs on desorption process

In order to better understand the K^+ competition towards Cs, Cs^+ desorption was studied by imposing various amounts of K on Cs doped K-free vermiculite (K(0)V) and K intercalated vermiculite (K(5)V). For this purpose, vermiculites were doped with Cs in trace level (6.6×10^{-6} mol/kg) and dispersed in solutions (K(0) and K(5) respectively) with added various concentrations of K.

For the K-free vermiculite doped with Cs in trace, Fig. 5 shows the mass balance of cations Ca^{2+} , Mg^{2+} , K^+ and Cs^+ (Fig. 5a and b) and the interlayer space evolution (Fig. 5c) as a function of the K^+ in solution at equilibrium. When the K(0) solution is used, the Cs desorption result is the same as the desorption isotherm (Fig. 4a). The Cs desorption amount (Fig. 5b) remains equal until 0.4 mmol/L K introduced without any significant exchange with Ca^{2+} and Mg^{2+} , and the interlayer space remains fully open (i.e. $d_{(001)}$ reflection at 14.6 Å in Fig. 5c). The Cs desorption increases with increasing K introduced between 0.7 to 5 mmol/L (Fig. 5b). The K^+ uptake is firstly balanced by Mg^{2+} then Ca^{2+} released in solution. The interlayer spaces are maintained at 14.6 Å without any significant mixed layer at 12.5 Å although K^+ introduced in solution represents at most 35% of the CEC but the adsorbed K represents only 5.3% of the

CEC. A large amount of K^+ is then necessary to extract no more than 4% of the adsorbed Cs from the vermiculite (i.e., $2.65 \cdot 10^{-7}$ mol/kg of Cs). This represents 3.7 to 27.9 times more than the K fertilizer amended ($250 \text{ mg/kg}_{\text{soil}} K_2O$) on Japanese soils (Kubo et al. 2015; Kato et al. 2015). Above 10 mmol/L K introduced (Fig. 5a), K^+ is largely loaded onto mineral and $Mg^{2+} > Ca^{2+}$ are released in solution while no Cs desorption occurs. From 10 mmol/L K introduced (i.e. 12.5 times less than conditioning solution for K(10)V), the structural analysis records the decrease in intensity and the spreading of the peak at 14.6 Å in favor of a peak at 12.5 Å, characteristic of a vermiculite /mica mixed layer (Kogure et al. 2012). The latter shifts towards 12 Å and spreads towards the large angles until reaching 10.8 Å for the highest K concentration. The interlayer space collapse is therefore evidenced with this structure change as reported by Kogure et al. (2012). This collapse is then related to the K adsorption corresponding to 11.4% of the sites available.

For the vermiculite initially loaded with K (K(5)V), the mass balances of cations Ca^{2+} , Mg^{2+} , K^+ and Cs^+ as a function of the K^+ in solution at equilibrium is given in Fig. 6a to 6c. This indicates a K^+ release balanced by a Ca^{2+} and Mg^{2+} uptake from solution when the contact solution has initially lower K concentration than the K(5) solution (Fig. 6b). In this case, the higher the K concentration, the lower the exchange with Ca and Mg. So, the $Mg > Ca$ exchange, mainly with K, as Cs desorption remains unchanged with the decrease of K concentration in solution. This results in the opening of the interlayer space of vermiculite (Fig. 6c), as expressed by the increase of diffraction peak intensity at 14.6 Å and a slight depletion of the mixed layer peak intensity at 12.5 Å ($d_{(001)}$ at 0 mmol/L K compared with that at 5 mmol/L K). Consequently, among the interlayer spaces, those containing exchangeable K seem particularly affected by this exchange. When the K(5) solution is used, the Cs desorption result is the same as the desorption isotherm (Fig. 4b). As K concentration becomes higher than the K(5) solution (> 5 mmol/L K), the solid uptakes K and releases first Mg^{2+} and Ca^{2+} . Then Cs desorption declines until stops between 10 and 25 mmol/L K concentration. As long as the Cs desorption occurs, no change of the interlayer space dimensions is recorded (see $d_{(001)}$ at 10 mmol/L K in Fig. 6c). When Cs desorption no longer occurs, characteristic peaks of mixed layer at 12.5 Å, 12 Å ($7.5^\circ 2\theta$) and the broad reflection at 10 Å ($8.6^\circ 2\theta$) indicate an increasing and mixing proportion of micaceous layer. This again evidences the collapse of the interlayers. Meanwhile, K adsorbed represents only 2.33% of the K(5)V CEC for 25 mmol/L K concentration. Hence, K intercalates and locks at least the vermiculite interlayer space which inhibits the release in solution of Cs mainly located at this structural site.

The role of K on trace Cs desorption is evidenced by mechanically scavenging Cs in the mineral structure of vermiculite and K incorporated vermiculites. Moreover, chemical competition between K and Cs is highlighted when the vermiculite interlayer space remains fully open and K is introduced in the medium. Then Cs selectivity at trace level of vermiculite and micaceous structures are higher than the one of K.

3.4. Mechanism of Cs sorption on vermiculite and micaceous structures

In order to establish the Cs sorption mechanism on vermiculite and micaceous structures in multi-cation media, cation exchange analyses were complemented with structural analyses on these structures. Indeed, Cs sorption isotherms and their corresponding cation mass balances showed that cation exchange takes place differently according to the K occupancy in the interlayer space of conditioned vermiculites. Structural site types, interlayer and external sites, involved in the Cs sorption are then inferred based on structural analyses by XRD (Fig. 7). These latter were performed on batch slurries from Cs desorption experiments at varying Cs concentrations for the K-free vermiculite and the K loaded vermiculites (Fig. 2, 4 and SI2).

Two distinct behaviors are evidenced depending on Cs concentration in contact with the various clay structures, synthesized in Fig. 8. At trace Cs level (until 10^{-6} mol/L of Cs), regardless the conditioned vermiculite, during Cs adsorption and desorption the original structure remains (Fig. 7) with only slight changes. Indeed, the (001) reflection of the K-free vermiculite expresses only one peak around 14.6 Å. Likewise, the XRD reflections of the K incorporated vermiculites show two peaks (Fig. 1). For reversible adsorption, the (001) reflections intensity at 14.6 Å decreases without significant enhancement of the mixed layer peak at 12.5 Å (except for K(10)V) and both reflections slightly shifts to larger angles. This can be related to a slight dehydration taking place in the interlayer space (Dzene et al. 2015). The (001) reflection intensities are higher at 10^{-6} mol/L Cs than at 10^{-9} mol/L Cs. This reflects the reincorporation of hydrated cations in the interlayer space subsequently to trace Cs desorption. This latter appears in larger amount at 10^{-6} mol/L Cs than at 10^{-9} mol/L Cs, confirmed by cation mass balances, and is made possible by the sufficiently opened interlayer space until a distance of 12.5 Å. However, the intensity and peak positions do not recover the original values, hence cations mixture have a whole lower hydration state in the interlayer space. Hence, the ratio between Ca to Mg in the interlayer space occupancy have changed. As Cs concentration increases above 10^{-5} mol/L in solution, the intensity of the vermiculite peak at 14.6 Å decreases, shifts towards large angles 2θ , and finally disappears to the benefit of mixed layer peak at 12.5 Å (Fig. 7) or less regardless of the initial mineral structure. This observation supports the hypothesis of an interlayer collapse subsequent to Cs incorporation and explains the partial reversibility of Cs sorption. The more vermiculite is initially charged with K, the smaller the $d_{(001)}$ value subsequent to Cs adsorption/desorption. Also, the more vermiculite are initially charged with K, the higher the amount of released Cs (i.e. 48.8 to 11.9% for K(10)V compared to 15.8 to 1.7% for K(0)V between 10^{-5} et 10^{-3} mol/L Cs). Moreover, Cs adsorption K_d (Fig. 1) decreases with increasing K loaded in the structure, and the Cs adsorption reversibility increases. Then, Cs desorption implies the role of external sites and the interlayer space when sufficiently opened. In K free media, the more Cs is absorbed, the more the collapse interlayer spaces and the fewer proportion of Cs released. K occupying the Cs selective sorption sites and being strongly incorporated in the structure, is not replaced by Cs.

When K disturbs the chemical equilibrium, the interlayer distance reduces to 10 Å (Figs. 5 and 6) upon Cs adsorption. Such a small distance is not reached by Cs introducing. Then, K is incorporated in the interlayer space by exchange with Ca^{2+} and Mg^{2+} and subsequently locks the Cs in trace specifically adsorbed on high selective and low capacity sites. This specific site should also be present on structural

basal site, by considering a sheet merging as shown by the disordered stacking on XRD pattern (broad reflection peak between 12 and 10 Å) (Motokawa et al. 2014 a, b). Similarly, to Cs (Motokawa et al. 2014 a, b), interlayer collapse subsequent to K incorporation may provide fresh planar adsorption sites for Cs. This is in accordance with the higher Cs desorption ability of K incorporated vermiculites. Due to its high exchange capacity, the interlayer space permits to load a large amount of Cs which remains free as long as the interlayer is sufficiently opened. Reactional scheme of the K⁺ impact on Cs⁺ exchange with Ca²⁺, Mg²⁺ and K⁺ on vermiculite and K intercalated vermiculites is displayed in Fig. 9.

The involvement of the specific structural site, usually named frayed edge site (FES) (Sawhney 1972) was investigated by artificially reducing the interlayer distance by incorporating K during the conditioning process. By reducing the vermiculite CEC with K fixation, it mimics a sequence between true vermiculite and vermiculitized-mica. Consequently, it was expected to increase the FES occurrence by letting available cations stay into the space close to the layer edge (Akemoto et al. 2020). High selectivity and low capacity sites are usually assimilated to the FES. So, this site type should be evidenced with Cs behavior at trace level. Partial Cs sorption reversibility in trace level (Fig. 1) is just evidenced on the highest K loaded vermiculite (K(10)V). In accordance with the structural analysis (Fig. 7c), the interlayer space reduction leads to constrain the diffusion of trace Cs adsorbed in the dehydrated interlayer space lower than 12.5 Å. So, Cs is adsorbed on basal, edge and interlayer space larger than 12.5 Å for this intercalated K vermiculite. Furthermore, Kd desorption is similar to Kd adsorption for other experimental conditions. Moreover, trace Cs adsorption decreases with K structural incorporation, while selectivity for Cs should increase. These results indicate that mixed layers at 12.5 Å, created by K incorporation, are not related to a structural FES site enhancement, responsible of the high affinity and sorption irreversibility. There is also no evidence that FES are really created under these operating conditions and that FES holds the chemical reactivity of the high selectivity and low capacity site.

Cs exchange sequences accounting for structural site involvement can be proposed by combining the results. As seen above, K⁺ in solution does not mainly interact in the ion exchange with Cs, given that the matrices are equilibrated with major cations in solution and intercalated K is mainly not exchangeable. Chemical composition of solutions reflects the sequence of cation exchange: at first, Mg²⁺ is exchanged with Cs, as Cs starts competing with Ca²⁺, this latter is released in solution. This explains the dehydration and secondly the reduction of the interlayer distance, in accordance with the cation hydration enthalpy ordered as Mg²⁺ > Ca²⁺ > K⁺ > Cs⁺, inversely to their cation radius (Noyes 1962; Yin et al. 2017). Consequently, K⁺ and Cs⁺ promote the decrease of the interlayer distance and are easily dehydrated resulting in the interlayer collapse (Sawhney 1972, Okumura et al. 2018, Motokawa et al. 2014 a,b). Part of the Cs is mechanically locked in the interlayer space (Kikushi et al. 2015). As the interlayer space opens, Mg²⁺, Ca²⁺ occupy both interlayer space and external sites. Because the hydration energy of Mg²⁺ is higher than that of Ca²⁺ (Yin et al., 2017), Ca²⁺ reincorporation is favored over Mg²⁺, which is consistent with the observed cation exchanges at high Cs concentration. Once the interlayer space is closed or reduced to 12 Å, hydrated Mg²⁺ appears too large to enter in shorter space (Okumura et al., 2018). This is evidenced by scanning the cation exchanges occurring at desorption step, especially for K

loaded vermiculites. As Cs adsorption leads to close the interlayer space, only few percent of adsorbed Cs may desorb. This Cs appears adsorbed on less affine sites. Ca^{2+} easily replaces the desorbed Cs^+ but Mg^{2+} is highly limited (Fig. 4 and SI2). So Mg^{2+} affinity is lower than Ca^{2+} for all sorption sites. In addition to K incorporated in the structure, the interlayer spaces show shorter distances. Consequently, desorbed Cs appears to come mainly from external sites (basal and edge site) when interlayer space is closed due to Cs adsorption. This interpretation is supported by the Robin et al. (2015) study on beidellite. These authors highlighted a preferred Ca^{2+} sorption on the external sites rather than Mg^{2+} . Cs adsorption reversibility is also dependent on the crystal structure. K/Cs competition occurs for K concentration thousand times higher than that of Cs. Indeed, high K amount is required to easily desorb Cs at trace concentration (above $7 \cdot 10^{-4}$ mol/L K in excess). Moreover, Cs is locked in the interlayer space with K incorporation. Consequently, K has a high selectivity for vermiculite and micaceous structures but remains lower than that of Cs.

4. Conclusions

Cs transfer to plant is highly dependent on the clay mineralogy of soil, especially as soils are enriched in micaceous minerals and vermiculite. To understand Cs bioavailability of radionuclides in soils, Cs sorption-desorption behavior on micaceous minerals and vermiculite was studied in chemical environment close to a natural soil. For this purpose, a sequence between vermiculite and weathered mica was produced by saturating a vermiculite with K at various content. Experiments involve simultaneous Cs^+ exchange with Ca^{2+} , Mg^{2+} and K^+ at thermodynamic equilibrium. By coupling sorption isotherms, cation mass balances and structural analysis by XRD, reactional scheme and involvement of structural sites on Cs adsorption and desorption on clay minerals in multi-cations solutions are inferred. Then K^+ competition on Cs^+ desorption is characterized by imposing various amounts of K on trace Cs doped vermiculite and K intercalated vermiculite. K concentrations were selected to mimic a K amendment in the fields, a K depletion in the solution due to plant uptake or weathering event, and to provide insight into the Cs location on the mineral structure.

Two Cs sorption behaviors were evidenced. At trace level, Cs exchange with Mg^{2+} and Ca^{2+} in a reversible adsorption process. External sites and interlayer sites remain available during exchange process whatever the amount of K incorporated in the structure. As Cs becomes to compete with major cations, Cs^+ replace firstly Mg^{2+} then Ca^{2+} . Cs^+ excess, as well as K^+ , leads to a reduction and to a collapse of the interlayer space. In this case, Mg^{2+} is excluded from the interlayer space and Cs located in this structural site is blocked and becomes non exchangeable. The residual exchangeable Cs is then assigned to the external sites. Lower Cs amount is loaded on micaceous structure than vermiculite. This is due to their lower cation exchange capacity resulting from K incorporation. In contrast, Cs adsorption on micaceous structure is more reversible, suggesting the dominant involvement of external sorption sites. Trace Cs^+ is seldom removed by K^+ . Cs is strongly adsorbed on the various matrix and a K/Cs ratio in solution of about thousand is needed to remobilize Cs. The present study provides strong evidence for the fact that interlayer sorption is responsible for the incomplete reversibility of Cs^+ sorption on clay minerals. In the

case of soil contamination by Cs, K⁺ amendment only leads to a weak enhancement of Cs desorption, more so for vermiculite than for micaceous minerals. Ca and Mg amount in natural systems will therefore affect Cs bioavailability.

Declarations

Acknowledgments

The authors acknowledge the French “Programme Investissement d’Avenir” (ANR 11-RSNR-0005 DEMETERRES, <https://anr.fr/ProjetIA-11-RSNR-0005>) and the French Alternative Energies and Atomic Energy Commission for their financial supports. The authors thank H el ene Isnard and Nathalie Coreau for their analytical support in ICP/MS and ion chromatography. Olivier Bildstein is acknowledged for his helpful English proofreading.

Author contribution

Conceptualization: Christelle Latrille. Literature search and data analysis: Christelle Latrille and Julien Dubus. Writing—original draft preparation: Christelle Latrille. Writing—review and editing: Christelle Latrille, Nathalie Prat-L eonhardt and Julien Dubus. Supervision: Christelle Latrille, Nathalie Prat-L eonhardt

Funding

The authors received financial support from the French “Programme Investissement d’Avenir” (ANR 11-RSNR-0005 DEMETERRES, <https://anr.fr/ProjetIA-11-RSNR-0005>) and the French Alternative Energies and Atomic Energy Commission.

Availability of data and material Not applicable.

Code availability Not applicable.

The authors have no relevant financial or non-financial interests to disclose.

The authors declare that they have no competing interests.

Ethics approval and consent to participate Not applicable.

Consent for publication Not applicable

References

1. Akemoto Y, Sakti SCW, Kan M, Tanaka S (2020) Interpretation of the interaction between cesium ion and some clay minerals based on their structural features. *Environ Sci Pollut Res*. <https://doi.org/10.1007/s11356-020-11476-7>

2. Benedicto A, Missana T, María Fernández A (2014) Interlayer collapse affects on cesium adsorption onto illite. *Environ Sci Technol* 48:4909–4915. <https://dx.doi.org/10.1021/es5003346>
3. Brindley GW, Brown G (1980) Interlayer and intercalation complexes of clay minerals. In: Brindley GW and Brown G (eds) *Crystal Structures of Clay Minerals and Their X-Ray Identification*, Mineralogical Society of Great Britain and Ireland, pp 305–356. <https://doi.org/10.1180/mono-5.3>
4. Brouwer E, Baeyens B, Maes A, Cremers A (1983) Cesium and rubidium ion equilibriums in illite clay. *J Phys Chem* 87:1213–1219
5. Cornell RM (1993) Adsorption of cesium on minerals: a review. *J Radioanal Nucl Chem* 171(2):483–500
6. Durrant CB, Begg JD, Kersting AB, Zavarin M (2018) Cesium sorption reversibility and kinetics on illite, montmorillonite, and kaolinite. *Sci Total Environ* 610–611:511–520. <http://dx.doi.org/10.1016/j.scitotenv.2017.08.122>
7. Dzene L, Tertre E, Hubert F, Ferrage E (2015) Nature of the sites involved in the process of cesium desorption from vermiculite. *J Colloid Interface Sci* 455:254–260. <http://dx.doi.org/10.1016/j.jcis.2015.05.053>
8. Fuller AJ, Shaw S, Peacock CL, Trivedi D, Small JS, Abrahamsen LG, Burke IT (2014) Ionic strength and pH dependent multi-site sorption of Cs onto a micaceous aquifer sediment. *Appl Geochem* 40:32–42. <http://dx.doi.org/10.1016/j.apgeochem.2013.10.017>
9. Kasar S, Mishra S, Omori Y, Sahoo SK, Kavasi N, Arae H, Sorimachi A, Aono T (2020) Sorption and desorption studies of Cs and Sr in contaminated soil samples around Fukushima Daiichi Nuclear Power Plant. *J Soils and Sediments* 20(1):392–403. <https://doi.org/10.1007/s11368-019-02376-6>
10. Kato N, Kihou N, Fujimura S, Ikeba M, Miyazaki N, Saito Y, Eguchi T, Itoh S (2015) Potassium Fertilizer and Other Materials as Countermeasures to Reduce Radiocesium Levels in Rice: Results of Urgent Experiments in 2011 Responding to the Fukushima Daiichi Nuclear Power Plant Accident. *Soil Sci Plant Nutr* 61(2):179–190. <https://doi.org/10.1080/00380768.2014.995584>
11. Kikuchi R, Mukai H, Kuramata C, Kogure T (2015) Cs-sorption in weathered biotite from Fukushima granitic soil. *J Min Petrol Sci* 110:126–134. <http://dx.doi.org/10.2465/jmps.141218>
12. Kitayama R, Yanai J, Nakao A (2020) Ability of micaceous minerals to adsorb and desorb caesium ions: effects of mineral type and degree of weathering. *Eur J Soil Sci* 71:1–13. <http://dx.doi.org/10.1111/ejss.12913>
13. Klika Z, Kraus L, Vopalka D (2007) Cesium uptake from aqueous solutions by bentonite: a comparison of multicomponent sorption with ion-exchange models. *Langmuir* 23:1227–1233. <http://dx.doi.org/10.1021/la062080b>
14. Kogure T, Morimoto K, Tamura K, Sato H, Yamagishi A (2012) XRD and HRTEM evidence for fixation of cesium ions in vermiculite clay. *Chem Lett* 41:380–382. <http://dx.doi.org/10.1246/cl.2012.380>
15. Kubo K, Nemoto K, Kobayashi H, Kuriyama Y, Harada H, Matsunami H, Eguchi T, Kihou N, Ota T, Keitoku S, Kimura T, Shinano T (2015) Analyses and countermeasures for decreasing radioactive

- cesium in buckwheat in areas affected by the nuclear accident in 2011. *Field Crops Res* 170:40–46. <http://dx.doi.org/10.1016/j.fcr.2014.10.001>
16. Kubo K, Fujimura S, Kobayashi H, Ota T, Shinano T (2017) Effect of soil exchangeable potassium content on cesium absorption and partitioning in buckwheat grown in a radioactive cesium-contaminated field. *Plant Prod Sci* 20(4):396–405. <https://doi.org/10.1080/1343943X.2017.1355737>
 17. Kubo K, Hirayama T, Fujimura S, Eguchi T, Nihei N, Hamamoto S, Takeuchi M, Saito T, Ota T, Shinano T (2018) Potassium behavior and clay mineral composition in the soil with low effectiveness of potassium application. *Soil Sci Plant Nutr* 64(2):265–271. <https://doi.org/10.1080/00380768.2017.1419830>
 18. Latrille C, Bildstein O (2022) Cs selectivity and adsorption reversibility on Ca-illite and Ca-vermiculite. *Chemosphere* 288(2):132582. <https://doi.org/10.1016/j.chemosphere.2021.132582>
 19. Lee SH (1973) Studies on the sorption and fixation of cesium by vermiculite. *J Korean Nucl Soc* 5(4):310–320
 20. Lee SH (1974) Studies on the sorption and fixation of cesium by vermiculite II. *J Korean Nucl Soc* 6(2):97–111
 21. Liu C, Zachara JM, Steve C, Smith A (2004) Cation exchange model to describe Cs⁺ sorption at high ionic strength in subsurface sediments at Hanford site, USA. *J Contam Hydrol* 68:217–238. [http://dx.doi.org/10.1016/S0169-7722\(03\)00143-8](http://dx.doi.org/10.1016/S0169-7722(03)00143-8)
 22. Maes E, Vielvoye L, Stone W, Delvaux B (1999) Fixation of radiocaesium traces in a weathering sequence mica → vermiculite → hydroxy interlayered vermiculite. *Eur J Soil Sci* 50:107–115. <https://doi.org/10.1046/j.1365-2389.1999.00223.x>
 23. Mishra S, Arae H, Sorimachi A, Hosoda M, Tokonami S, Ishikawa T, Sahoo SK (2015) Distribution and retention of Cs radioisotopes in soil affected by Fukushima nuclear plant accident. *J Soils Sediments* 15:374–380. <https://doi.org/10.1007/s11368-0.14-0985-2>
 24. Missana T, Benedicto A, Garcia-Gutierrez M, Alonso U (2014) Modeling cesium retention onto Na-, K- and Ca-smectite: effects of ionic strength, exchange and competing cations on the determination of selectivity coefficients. *Geochim Cosmochim Acta* 128:266–277. <https://dx.doi.org/10.1016/j.gca.2013.10.007>
 25. Morimoto K, Kogure T, Tamura K, Tomofuji S, Yamagishi A, Sato H (2012) Desorption of Cs⁺ ions intercalated in vermiculite clay through cation exchange with Mg²⁺ ions. *Chem Lett* 41(12):1715–1717. <https://dx.doi.org/10.1246/cl.2012.1715>
 26. Motokawa R, Endo H, Yokoyama S, Ogawa H, Kobayashi T, Suzuki S, Yaita T (2014a) Mesoscopic structures of vermiculite and weathered biotite clays in suspension with and without cesium ions. *Langmuir* 30:15127–15134. <https://dx.doi.org/10.1021/la503992p>
 27. Motokawa R, Endo H, Yokoyama S, Nishitsuji S, Kobayashi T, Suzuki S, Yaita T (2014b) Collective structural changes in vermiculite clay suspensions induced by cesium ions. *Sci Rep* 4:6585. <https://dx.doi.org/10.1038/srep06585>

28. Mukai H, Hirose A, Motai S, Kikuchi R, Tanoi K, Nakanishi TM, Yaita T, Kogure T (2016) Cesium adsorption/desorption behavior of clay minerals considering actual contamination conditions in Fukushima. *Sci Rep* 6:21543. <https://dx.doi.org/10.1038/srep21543>
29. Mukai H, Tamura K, Kikuchi R, Takahashi Y, Yaita T, Kogure T (2018) Cesium desorption behavior of weathered biotite in Fukushima considering the actual radioactive contamination level of soils. *J Environ Radioact* 190–191:81–88. <https://doi.org/10.1016/j.jenvrad.2018.05.006>
30. Murota K, Saito T, Tanaka S (2016) Desorption kinetics of cesium from Fukushima soils. *J Environ Radioact* 153:134–140. <https://dx.doi.org/10.1016/j.jenvrad.2015.12.013>
31. Murota K, Tanoi K, Ochiai A, Utsunomiya S, Saito T (2020) Desorption mechanisms of cesium from illite and vermiculite. *Appl Geochem* 123:104768. <https://doi.org/10.1016/j.apgeochem.2020.104768>
32. Nakao A, Ogasawara S, Sano O, Ito T, Yanai J (2014) Radiocesium sorption in relation to clay mineralogy of paddy soils in Fukushima, Japan. *Sci Total Environ* 468–469:523–529. <https://doi.org/10.1016/j.scitotenv.2013.08.062>
33. Noyes RM (1962) Thermodynamics of ion hydration as a measure of effective dielectric properties of water. *J Am Chem Soc* 84:513–522
34. Ogasawara S, Eguchi T, Nakao A, Fujimura S, Takahashi Y, Matsunami H, Tsukada H, Yanai J, Shinano T (2019) Phytoavailability of ¹³⁷Cs and stable Cs in soils from different parent materials in Fukushima, Japan. *J Environ Radioact* 198:117–125. <https://doi.org/10.1016/j.jenvrad.2018.12.028>
35. Ohnuki T, Kozai N (2013) Adsorption behavior of radioactive cesium by non-mica minerals. *J Nucl Sci Technol* 50(4):369–375. <https://dx.doi.org/10.1080/00223131.2013.773164>
36. Okumura M, Kerisit S, Bourg IC, Lammers LN, Ikeda T, Sassi M, Rosso KM, Machida M (2018) Radiocesium interaction with clay minerals: theory and simulation advances Post-Fukushima. *J Environ Radioact* 189:135–145. <https://doi.org/10.1016/j.jenvrad.2018.03.011>
37. Park SM, Alessi DS, Baek K (2019) Selective adsorption and irreversible fixation behavior of Cesium onto 2:1 layered clay mineral: a mini review. *J Hazard Mater* 369:569–576. <https://doi.org/10.1016/j.jhazmat.2019.02.061>
38. Robin V, Tertre E, Beaufort D, Regnault O, Sardini P, Descostes M (2015) Ion exchange reactions of major inorganic cations (H⁺, Na⁺, Ca²⁺, Mg²⁺ and K⁺) on beidellite: Experimental results and new thermodynamic database. Toward a better prediction of contaminant mobility in natural environments. *Appl Geochem* 59:74–84. <https://dx.doi.org/10.1016/j.apgeochem.2015.03.016>
39. Sakalidis CA, Misaelides P, Alexiades CA (1988) Caesium selectivity and fixation by vermiculite in the presence of various competing cations. *Environ Pollut* 52:67–79
40. Sawhney BL (1964) Sorption and fixation of microquantities of cesium by clay minerals: effect of saturation cations. *Soil Sci Soc Am J* 28(2):183–186. <https://doi.org/10.2136/sssaj1964.03615995002800020017x>
41. Sawhney BL (1972) Selective sorption and fixation of cations by clay minerals - review. *Clay Clay Miner* 20(2):93–100

42. Siroux B, Latrille C, Beaucaire C, Petcut C, Tabarant M, Benedetti MF, Reiller PE (2021) On the use of a multi-site ion-exchange model to predictively simulate the adsorption behaviour of strontium and caesium onto French agricultural soils. *Appl Geochem* 132:105052. <https://doi.org/10.1016/j.apgeochem.2021.105052>
43. Tamura K, Sato H, Yamagishi A (2015) Desorption of Cs⁺ ions from a vermiculite by exchanging with Mg²⁺ ions: effects of Cs⁺-capturing ligand. *J Radioanal Nucl Chem* 303:2205–2210. <https://dx.doi.org/10.1007/s10967-014-3744-3>
44. Wissocq A, Beaucaire C, Latrille C (2018) Application of the multi-site ion exchanger model to the sorption of Sr and Cs on natural clayey sandstone. *Appl Geochem* 93:167–177. <https://doi.org/10.1016/j.apgeochem.2017.12.010>
45. Yamamoto T, Takigawa T, Fujimura T, Shimada T, Ishida T, Inoue H, Takagi S (2019) Which types of clay minerals fix cesium ions effectively? the “cavity-charge matching effect”. *Phys Chem Chem Phys* 21:9352–9356. <https://doi.org/10.1039/c9cp00457b>
46. Yin X, Wang X, Wu H, Takahashi H, Inaba Y, Ohnuki T, Takeshita K (2017) Effects of NH₄⁺, K⁺, Mg²⁺, and Ca²⁺ on the cesium adsorption/desorption in binding sites of vermiculitized biotite. *Environ Sci Technol* 51:13886–13894. <https://doi.org/10.1021/acs.est.7b04922>

Figures

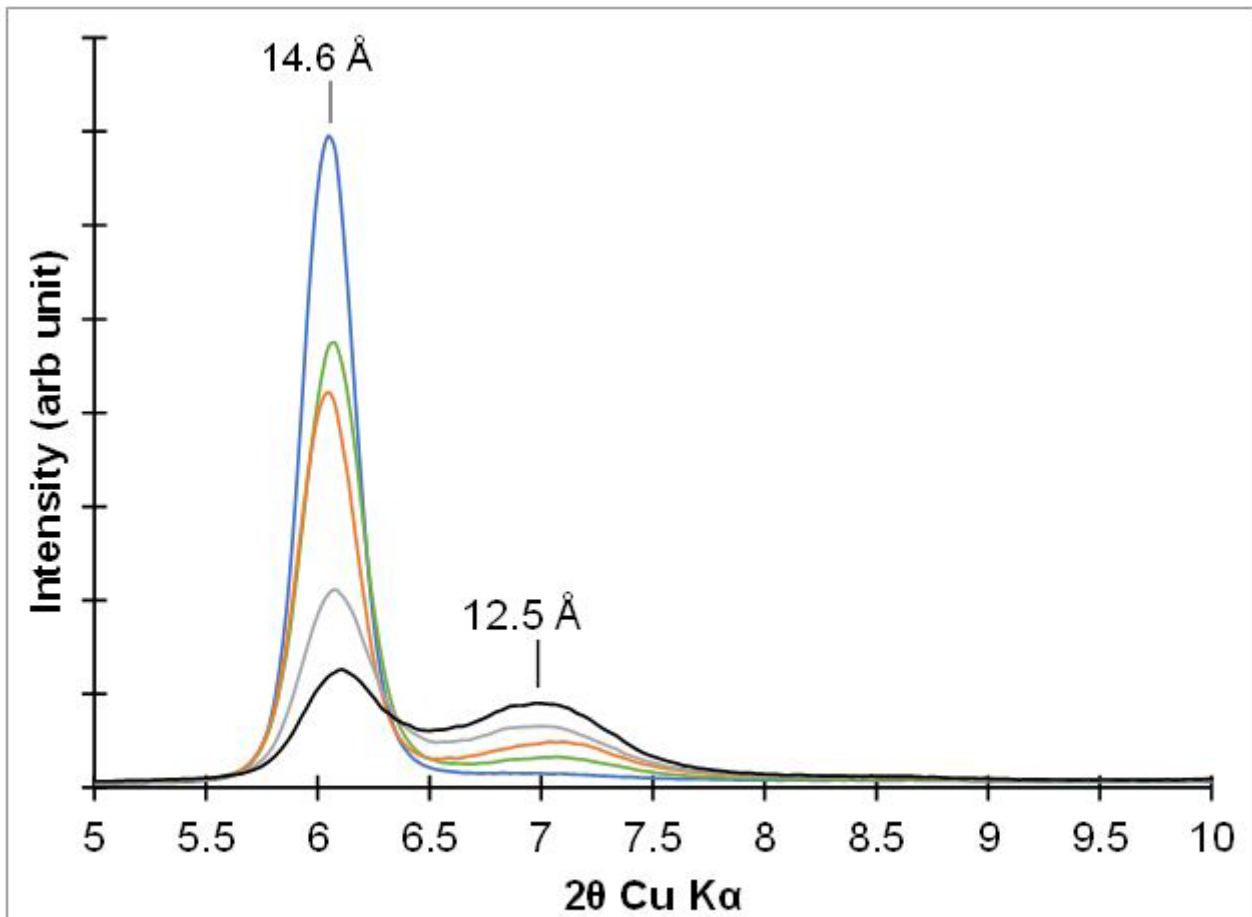


Figure 1

X-ray diffraction patterns of the five conditioned vermiculites

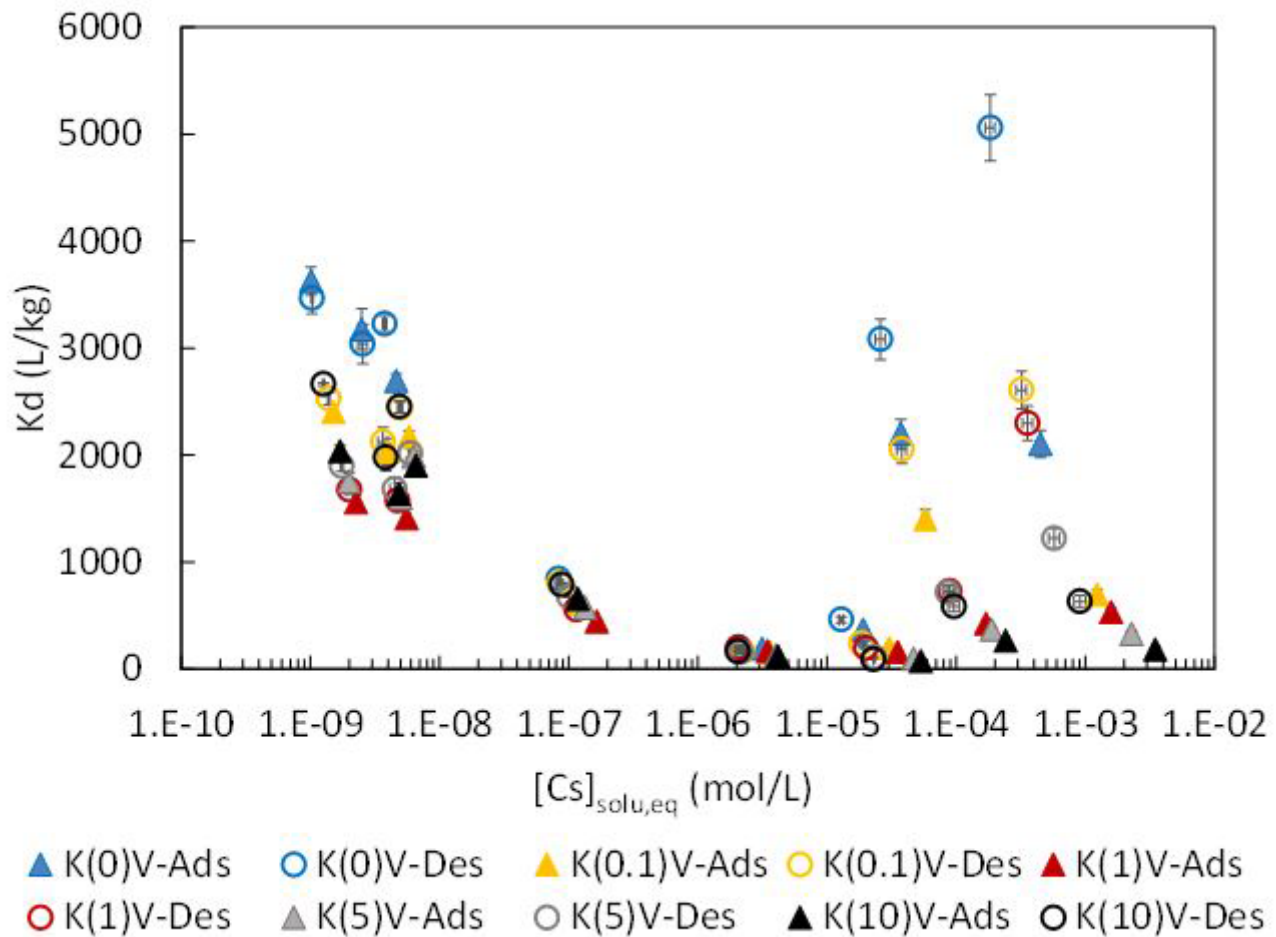


Figure 2

The K_d distribution coefficients vs. the $[Cs]_{solu,eq}$ concentration at equilibrium on five conditioned vermiculites K(x)V for Cs adsorption (triangle) and desorption (circle) isotherms. K(x) refers to the K concentration of solutions with $x = 0$ mol/L (blue), 0.1 mmol/L (yellow), 1 mmol/L (red), 5 mmol/L (grey) and 10 mmol/L (black) (pH = 5.6). The error bars correspond to the uncertainty of K_d value.

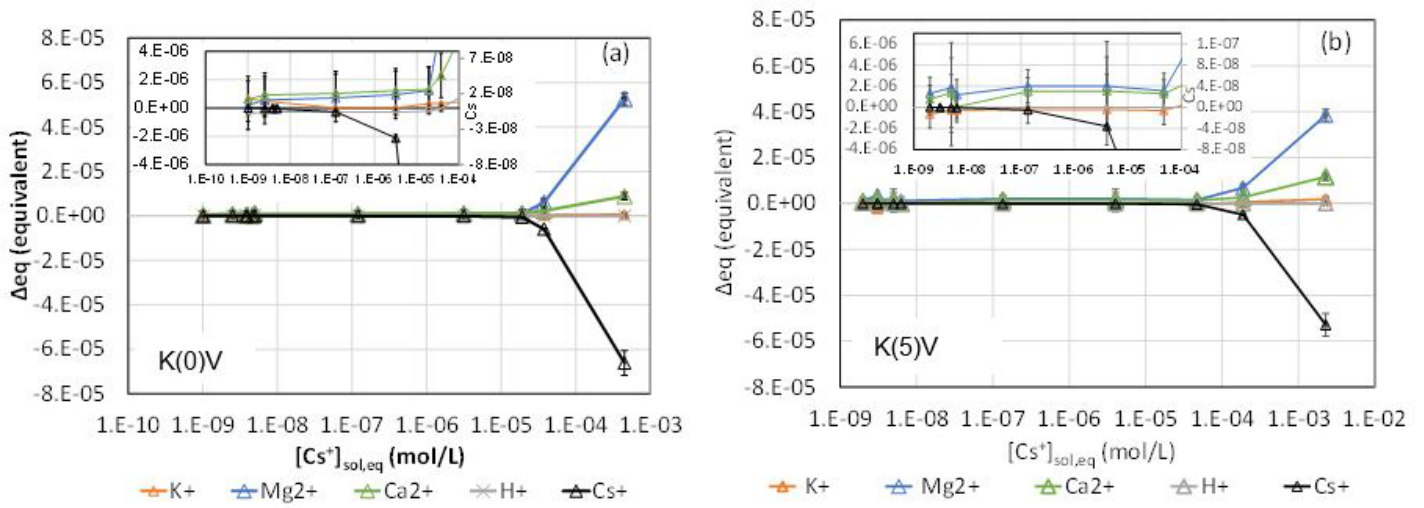


Figure 3

Mass balances of Cs^+ , K^+ , Ca^{2+} , Mg^{2+} and H^+ in solution at equilibrium from adsorption step performed with (a) the K-free vermiculite (K(0)V) and (b) the vermiculite at 27% occupancy by K (K(5)V).

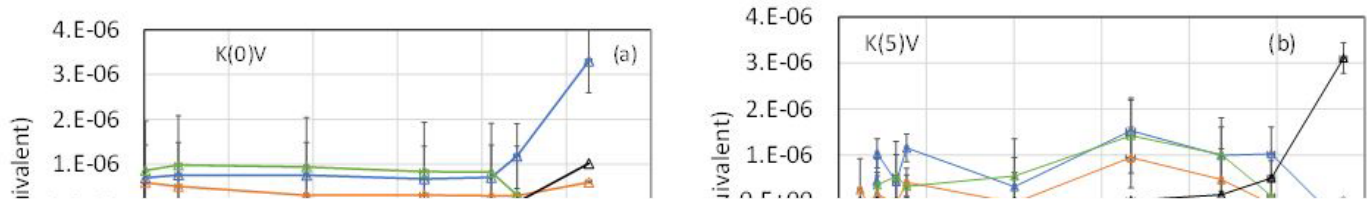


Figure 4

Mass balances of Cs^+ , K^+ , Ca^{2+} , Mg^{2+} and H^+ in solution at equilibrium from desorption step performed with (a) the vermiculite exempt of K (K(0)V) and (b) the vermiculite at 27% occupancy by K (K(5)V).

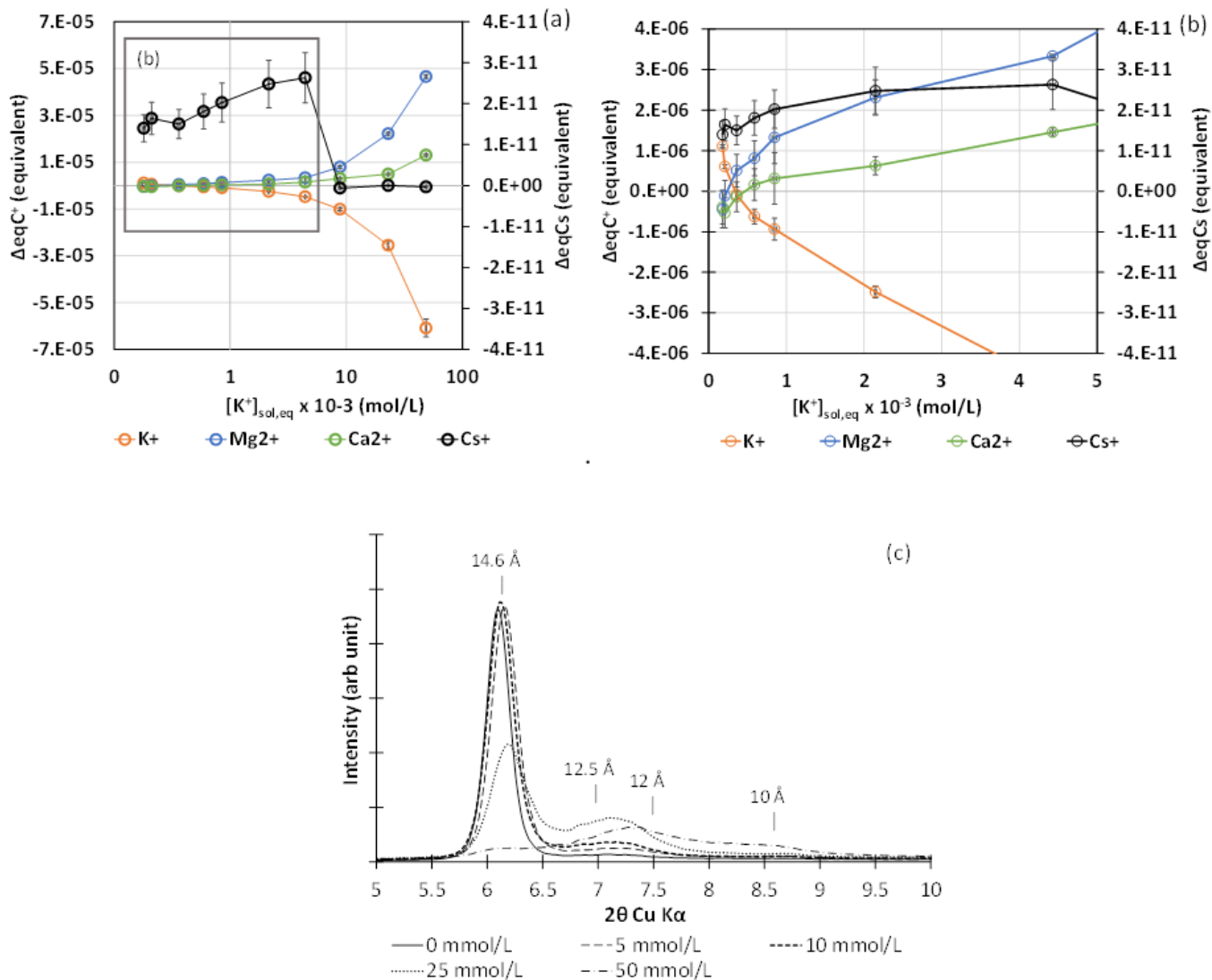


Figure 5

Mass balances of Cs⁺, K⁺, Ca²⁺ and Mg²⁺ in solution during Cs desorption from K-free vermiculite (K(0)V) doped with 6.62 10⁻⁶ mol/kg Cs vs. K⁺ concentration in solution (a) and (b); (c) XRD analyses of samples submitted to 0, 5, 10, 25 and 50 mmol/L K.

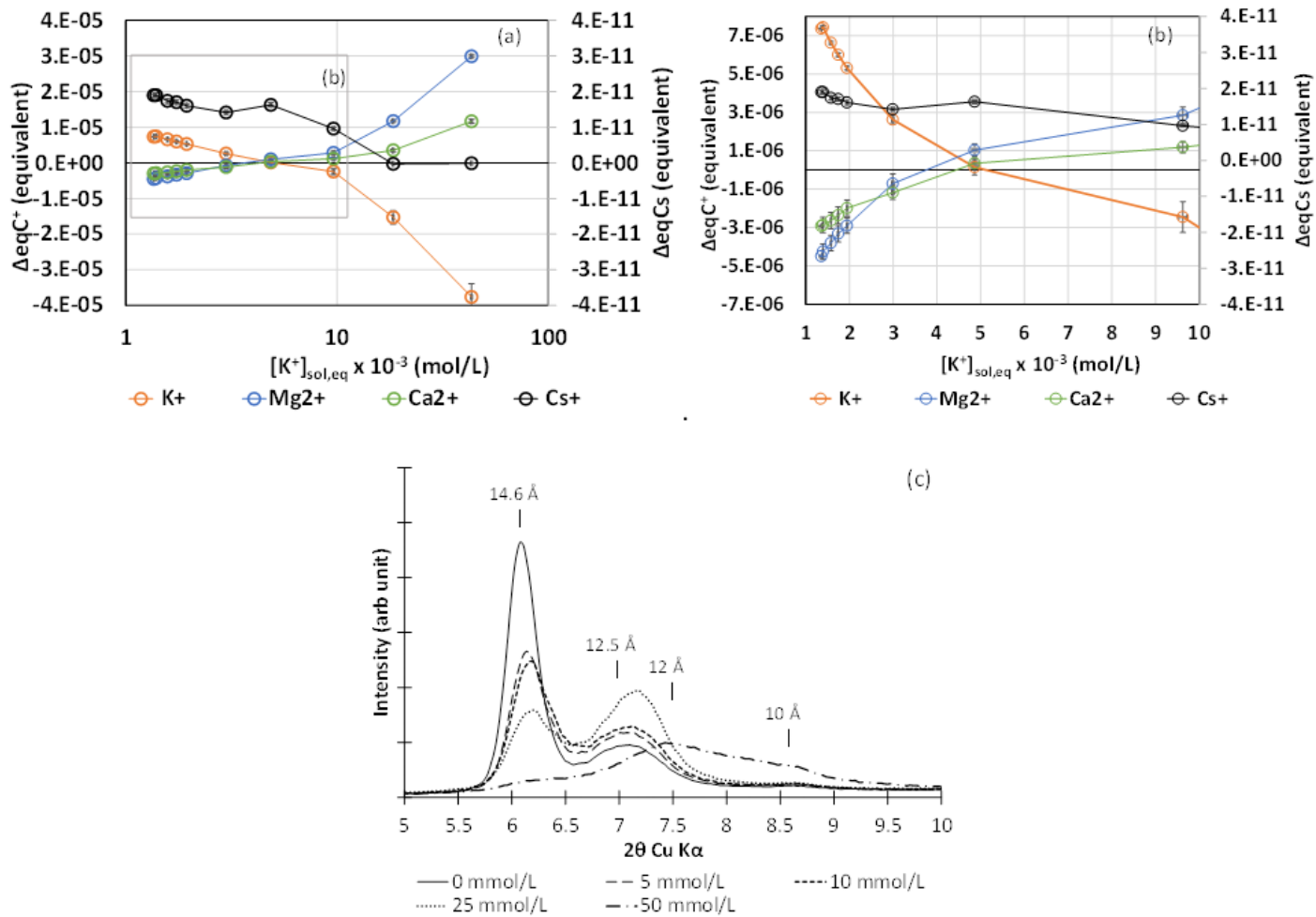


Figure 6

Mass balances of Cs^+ , K^+ , Ca^{2+} and Mg^{2+} in solution during Cs desorption from vermiculite K loaded (K(5)V) and doped with $6.62 \times 10^{-6} \text{ mol/kg Cs}$ vs. K^+ concentration in solution (a) and (b); (c) XRD analyses of samples submitted to 0, 5, 10, 25 and 50 mmol/L K^+ .

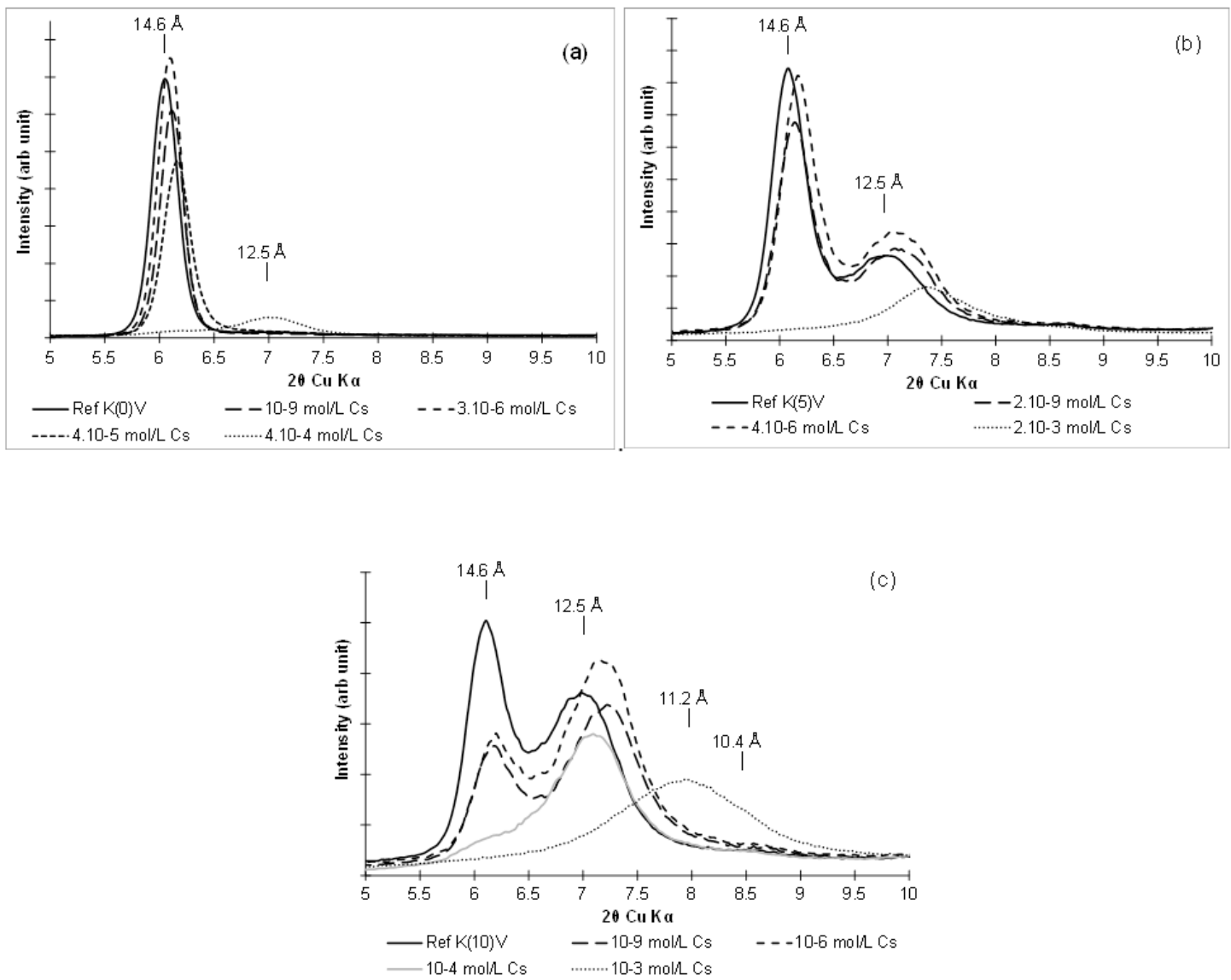


Figure 7

XRD patterns of (001) reflection from K(0)V (a), K(5)V (b) and K(10)V (c) samples in function of Cs concentration in solution at equilibrium after the desorption process. The $d(001)$ values are indicated in Angströms.

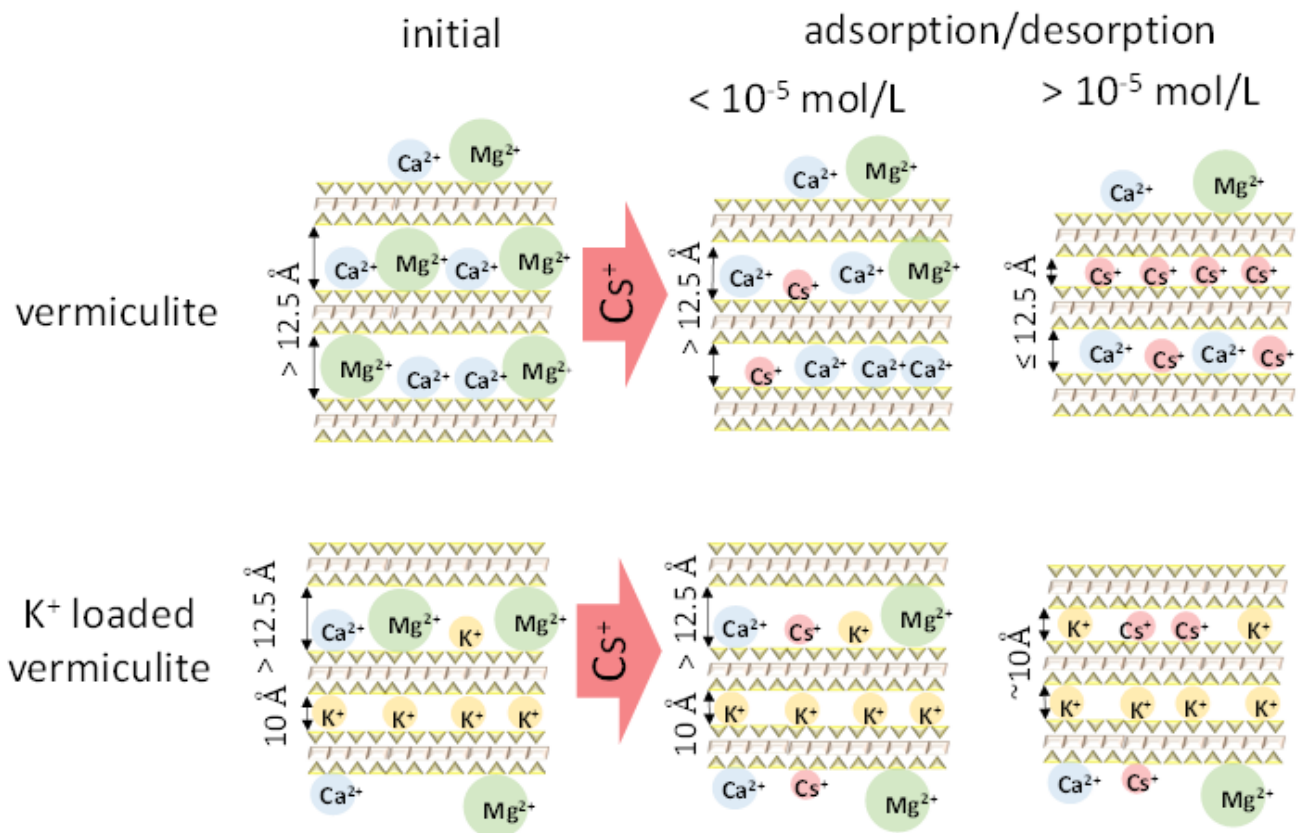


Figure 8

Reactional conceptual scheme of Cs⁺ exchange with Ca²⁺, Mg²⁺, K⁺ on vermiculite and K intercalated vermiculites.

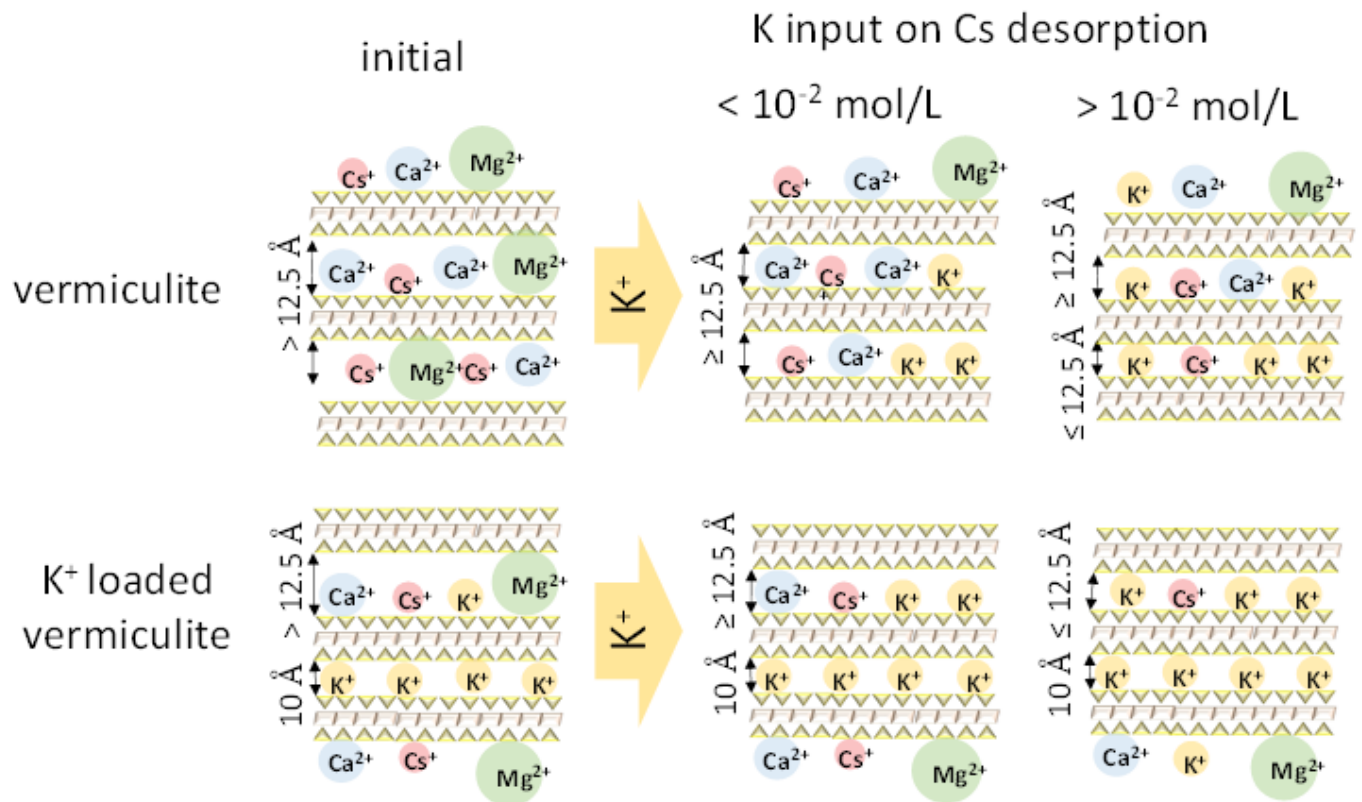


Figure 9

Reactional conceptual scheme of the K^+ impact on Cs^+ exchange with Ca^{2+} , Mg^{2+} and K^+ on vermiculite and K intercalated vermiculites.

Supplementary Files

This is a list of supplementary files associated with this preprint. Click to download.

- [Supplementaryinformations.docx](#)